The American Journal of Pathology, Vol. 175, No. 3, September 2009

DOI: 10.2353/ajpath.2009.080832

Cell Injury, Repair, Aging and Apoptosis

Functional Consequences of Mitochondrial DNA Deletions in Human Skin Fibroblasts

Increased Contractile Strength in Collagen Lattices Is Due to Oxidative Stress-Induced Lysyl Oxidase Activity

Marc Majora,* Tanja Wittkampf,* Bianca Schuermann,* Maren Schneider,* Susanne Franke,* Susanne Grether-Beck,* Ekkehard Wilichowski,† Françoise Bernerd,‡ Peter Schroeder,* and Jean Krutmann*

From the Institut fuer Umweltmedizinische Forschung, the Heinrich-Heine University Duesseldorf gGmbH, Duesseldorf, Germany; the Department of Paediatrics and Neuropaediatrics,† University of Goettingen, Goettingen, Germany; and L'Oréal Recherche,‡ Clichy, Paris, France*

Deletions within the mitochondrial DNA (mtDNA) are thought to contribute to extrinsic skin aging. To study the translation of mtDNA deletions into functional and structural changes in the skin, we seeded human skin fibroblasts into collagen gels to generate dermal equivalents. These cells were either derived from Kearns-Sayre syndrome (KSS) patients, who constitutively carry large amounts of the UV-inducible mitochondrial common deletion, or normal human volunteers. We found that KSS fibroblasts, in comparison with normal human fibroblasts, contracted the gels faster and more strongly, an effect that was dependent on reactive oxygen species. Gene expression and Western blot analysis revealed significant upregulation of lysyl oxidase (LOX) in KSS fibroblasts. Treatment with the specific LOX inhibitor β-aminopropionitrile decreased the contraction difference between KSS and normal human fibroblast equivalents. Also, addition of the antioxidant *N*-tert-butyl-α-phenylnitrone reduced the contraction difference by inhibiting collagen gel contraction in KSS fibroblasts, and both β-aminopropionitrile and *N*-tert-butyl-α-phenylnitrone diminished LOX activity. These data suggest a causal relationship between mtDNA deletions, reactive oxygen species production, and increased LOX activity that leads to increased contraction of collagen gels. Accordingly, increased LOX expression was also observed *in vivo* in photoaged human and mouse skin. Therefore, mtDNA deletions in human fibroblasts may lead to functional and structural alterations of the skin. ***(Am J Pathol 2009, 175:1019–1029; DOI: 10.2353/ajpath.2009.080832)***

Oxidative stress can damage biological macromolecules including lipids, proteins, and DNA.[1,2] In this regard, mitochondrial DNA (mtDNA), a circular molecule comprising 16,569 bp in human cells, is particularly vulnerable, due to its close proximity to the mitochondrial electron transport chain as the major intracellular source of reactive oxygen species (ROS), its lack of histones, and a limited repertoire of DNA repair capacity.[3,4] Mitochondrial DNA encodes for 13 essential components of the electron transport chain, 22 tRNAs and 2 rRNAs involved in their translation. As a consequence, mutations of mtDNA including point mutations and large scale deletions interfere with mitochondrial physiology and result in cellular dysfunction. So far, more than 100 point mutations associated with a heterogeneous spectrum of pathological abnormalities have been reported.[5] Large scale deletions such as the 4977 bp-containing common deletion are found in a number of mitochondrial disorders that can occur sporadically or can be inherited maternally. The best known mitochondrial disease associated

Supported by the "Deutsche Forschungsgemeinschaft (DFG)" Collaborative Research Center (SFB) 728 and Graduate School GK 1033. L'Oréal Recherche is acknowledged for exclusive financial support of the *in vitro* experiments performed in this study. They have not been involved in the *in vivo* part of the study.

M.M. and T.W. contributed equally to this work.

Accepted for publication June 3, 2009.

Present address of T.W.: Department of General Pediatrics, Muenster University Children's Hospital, University of Muenster, Germany.

Address reprint requests to Prof. Dr. Jean Krutmann, Institut fuer umweltmedizinische Forschung (IUF) at the Heinrich-Heine University Duesseldorf gGmbH, Duesseldorf, Germany. Auf'm Hennekamp 50. 40225 Duesseldorf, Germany. E-mail: krutmann@uni-duesseldorf.de.

with the common deletion is Kearns-Sayre syndrome (KSS). KSS appears to be a sporadical disease that is clinically characterized by skeletal muscle weakness, progressive ptosis, external ophthalmoplegia, retinopathy, cardiac conduction defects, and brain damage.[6]

Mutations of mtDNA are not only found in mitochondrial diseases but are also frequently detected in aged tissues with high energy demands such as skeletal muscle, heart, and neurons,[7–10] and it has therefore been proposed that mtDNA mutations are causally related to the aging process. At least for point mutations, this assumption has recently been supported by a number of elegant studies using mtDNA mutator mice.[11,12] The precise molecular mechanisms, however, through which mtDNA mutations in general and mtDNA deletions in particular contribute to the aging process of a given tissue, are not yet understood.

In this regard recent studies suggest a role for large scale deletions of mtDNA in premature (=extrinsic) aging of human skin.[13–15] Among all environmental factors, solar ultraviolet (UV) radiation is the most important in extrinsic skin aging, a process accordingly also termed photoaging.[16] In photoaged skin, the amount of large scale deletions of mtDNA such as the common deletion is increased up to tenfold, as compared with sun-protected skin of the same individuals.[17] Also, chronic exposure to UV radiation induces large scale deletions of mtDNA in human skin fibroblasts *in vitro* as well as *in vivo*,[10,15] and UV-induced mtDNA mutagenesis is associated with a decline of mitochondrial functions.[18] In human skin, UV-induced deletions were found to persist for years and their levels increased after cessation of UV irradiation even in the absence of further exposures.[15]

In the present study, we have addressed the question how the presence of mtDNA deletions in human skin fibroblasts translates into structural and functional alterations in human skin by using dermal equivalents. Dermal equivalents can be generated by seeding human skin fibroblasts into a collagen gel, which is then remodeled and contracted by these cells within several days. After finishing the contraction process, the dermal equivalents can be kept in culture for several weeks. This organotypic model system has been shown to closely resemble the dermal compartment of living human skin[19] and has extensively been used in cutaneous biological research.[20–23] To exclude that any of the observed changes result from UV radiation-induced effects that are independent of the generation of large scale mtDNA deletions, either unirradiated normal healthy human skin fibroblasts (NHFs) or unirradiated human skin fibroblasts from KSS patients, which constitutively carry the UV-inducible common deletion, were used to generate dermal equivalents. Here, we report on differences between NHFs and KSS fibroblasts that occur within the initiation phase of the dermal equivalents, ie, the first 4 days of culture.

Materials and Methods

Cells and Culture Conditions

Primary KSS skin fibroblasts were derived from skin biopsies obtained from a 9- and a 10-year-old female KSS patient. Primary NHFs were isolated from skin samples obtained from a 7- and an 8-year old healthy donor. The study was approved by the local ethics committee. Cells were cultivated in Dulbecco's minimum essential minimal medium (PAA, Pasching, Austria) supplemented with 10% fetal calf serum, 1% L-glutamine, 1% antibiotic/antimycotic, 1% sodium pyruvate, and 200 μmol/L uridine (all supplements from Invitrogen, Karlsruhe, Germany except for uridine, which was purchased from Sigma, Taufkirchen, Germany) in a humidified atmosphere containing 5% CO_2 and used for experiments in passages between 8 and 16. Cells were matched for passage numbers for each experiment.

Generation of Dermal Equivalents

Dermal equivalents were generated as previously described.[24,25] Fibroblasts were harvested and resuspended in Eagle's minimum essential medium containing 25 mmol/L HEPES and supplemented with 10% fetal calf serum, 1% L-glutamine, 1% sodium pyruvate, 1% non-essential amino acids, 0.2% penicillin/streptomycin, 0.1% antibiotic/antimycotic. A total of 1×10^6 cells were mixed with 10.5 mg of native collagen I derived from the dermal compartment of calf hinds that had been extracted with acetic acid (Symatese Biomateriaux; Chaponost, France) and Earle's minimal essential medium (Biochrom AG; Berlin, Germany) supplemented with 3.5% $NaHCO_3$, 8% 0.1 N NaOH, 14% fetal calf serum, 0.63% L-glutamine, 0.63% sodium pyruvate, 0.63% non-essential amino acids, 0.06% penicillin/streptomycin, 0.03% antibiotic/antimycotic, in a total volume of 7 ml and poured into a Petri dish (Becton Dickinson; Heidelberg, Germany). Collagen concentration was 1.5 mg/ml. Telopeptides were retained during the manufactural isolation of the collagen. The diameter of the collagen gel was measured at the indicated time points until 96 hours after synthesis and subsequently the surface area was calculated. At the beginning of the experiment (time point 0) the area was considered to be 100%.

For some experiments, contraction was performed under hypoxic conditions. For this purpose, an anoxy chamber (IUL Instruments GmbH; Königswinter, Germany) containing an oxygen-free atmosphere consisting of 80% N_2, 10% CO_2, and 10% H_2 was used. To deplete residual oxygen in the culture flasks, cells were grown in the anoxy chamber 48 hours before being used for experiments. Culture medium was degassed before for 2 hours and equilibrated for additional 12 hours in the anoxy chamber. Additionally, all used media for contraction were treated equally. Generation of dermal equivalents was performed in the anoxy chamber and equivalents were cultured in the chamber until the end of the experiment.

In some experiments contraction was analyzed in the presence of β-aminoproprionitrile (BAPN) or *N*-tert-butyl-α-phenylnitrone (PBN), which were both purchased from Sigma. In these experiments cells were incubated for 24 hours in medium containing 10 mmol/L BAPN. Application of this rather high concentration was found to be necessary to inhibit contraction of KSS dermal equiva-

lents robustly and reproducible. No increased apoptosis rate was found among NHF and KSS fibroblasts cultivated for 48 hours in the presence of 10 mmol/L BAPN as determined by annexin V/7-Aminoactinomycin D staining (data not shown). BAPN or PBN (10 mmol/L) were also added directly to the contraction medium. A PBN concentration of 10 mmol/L was found to reduce cytosolic ROS levels in NHF and KSS fibroblasts by 25% (data not shown). We also did not notice increased apoptosis in NHF and KSS fibroblasts cultivated with 10 mmol/L PBN for 24 hours (data not shown).

Contraction experiments were performed with fibroblasts from two NHF and KSS donors. Results are presented as relative gel areas and for sake of clarity data are pooled for both NHF and KSS equivalents.

Measurement of ROS

Cytosolic ROS production in fibroblasts was measured using 2,7-dichlorofluorescein diacetate (DCFDA; Invitrogen). Cells were incubated in PBS containing 100 μmol/L DCFDA in 24-well plates and DCF fluorescence was monitored spectrofluorometrically (excitation: 485 nm; emission: 538 nm) using a Fluoroskan Ascent (Labsystems, Helsinki, Finland). For assessment of mitochondrial superoxide production cells were incubated in PBS containing 5 μmol/L MitoSOX (Invitrogen). Cells were washed with PBS three times and MitoSOX fluorescence was measured spectrofluorometrically. After measurement, cells were detached from plates by incubation with trypsin and counted. Fluorescence intensity was normalized to cell numbers for determination of ROS levels.

Real-Time PCR

DNA was extracted from the cells using the QIAamp DNA Mini Kit (Qiagen, Hilden Germany) following the instructions of the manufacturer. Concentration of DNA was measured photometrically. Semiquantitative measurement of total mitochondrial DNA (mtDNA) and the level of the mitochondrial Common Deletion were performed using an ABI Prism 7000 sequence detection system (Applied Biosystems, Foster City, USA) according to Koch et al.[26] The 83 bp fragment serving as an internal standard for quantification of total mtDNA was amplified by using the primers 5′-GATTTGGGTACCACCCAAGTATTG-3′ and 5′-AATATTCATGGTGGCTGGCAGTA-3′. Presence of the Common Deletion was verified by amplification of a 108 bp fragment using the primers 5′-ACCCCCATACTCCTTACACTATTCC-3′ and 5′-AAGGTATTCCTGCTAATGCTAGGCT-3′. Amplification was performed in a 25 μl reaction volume with 1× Platinum SYBR Green qPCR SuperMix-UDG (Invitrogen) containing 100 ng DNA and 50 nmol/L of each primer. PCR conditions were 2 minutes at 50°C, 10 minutes at 95°C, followed by 50 cycles of 15 seconds at 95°C and 1 minute at 60°C. Level of the Common Deletion was calculated in comparison with integer mtDNA.

RNA isolation of fibroblasts was performed using TRIzol reagent (Invitrogen) according to the instructions of the manufacturer. For RNA isolation from skin biopsies the RNeasy fibrous tissue mini kit (Qiagen) was used. RNA quantity and quality were verified photometrically. Poly(dT)-primed cDNA was synthesized after DNase I treatment using 1 μg of total RNA in a reaction containing 80 U RNaseOut, 400 U reverse transcriptase, 10 mmol/L dithiothreitol, and 100 μmol/L of each dNTP (all reagents were obtained from Invitrogen). Expression of lysyl oxidase (LOX) was analyzed by semiquantitative real-time PCR. For human samples the LOX-specific primers 5′-ACATCCTGTGACTATGGCTACC-3′ and 5′-CTGGGGTTTACACTGACCTTTA-3′ were used and expression was normalized to 18S ribosomal RNA (5′-GCCGCTAGAGGTGAAATTCTTG-3′ and 5′-CATTCTTGGCAAATGCTTTCG-3′). For murine samples the LOX primers 5′-CAACATTACCACAGCATGGA-3′ and 5′-ACCAGGTAGCTGGGGTTTAC-3′ were used and the expression was normalized to RPS6 (5′-ATTCCTGGACTGACAGACAC-3′ and 5′-GTTCTTCTTAGTGCGTTGCT-3′). Transcripts were amplified for 40 cycles of 20 seconds at 94°C followed by 20 seconds at 56°C and 45 seconds at 72°C.

Western Blot

For Western blot analysis, cells were homogenized in lysis buffer (125 mmol/L Tris, 4% SDS, 20% glycerin, 100 mmol/L dithiothreitol). Equal amounts of protein were separated by SDS-polyacrylamide gel electrophoresis and transferred to nitrocellulose membranes. Blots were blocked with 5% skim milk in TBS-Tween 20 (0.002%; TBS-T) buffer for 1 hour at room temperature and rinsed with TBS-T. They were incubated overnight at 4°C with a goat anti-lysyl oxidase polyclonal antibody (Santa Cruz, Heidelberg, Germany) followed by washing in TBS-T. Subsequently, blots were incubated with an anti-goat horseradish peroxidase-conjugated secondary antibody for 1 hour at room temperature and washed with TBS-T. As a horseradish peroxidase substrate, Chemiglow reagent (Biozym Scientific, Hess. Oldendorf, Germany) was used. For detection and quantification of the protein bands a charge-coupled device camera (Fluorchem 8900 imaging system, α Innotech, San Leandro, CA) and the AlphaEaseFC software were used.

Immunohistological Analysis

For immunohistological analysis, samples of dermal equivalents were embedded in optimal cutting temperature compound (Leica Microsystems, Nussloch, Germany) and snap-frozen with liquid nitrogen. Sections were cut at 8 μm using a CM3050 S Cryostat (Leica Microsystems) and fixed in ice-cold acetone. The following antibodies (Abs) were used in this study: anti-Pyd [trifunctional pyridinium crosslink, pyridinoline (Pyd)] Ab (Osteomedical GmbH, Buende, Germany), anti-Vimentin Ab (Monosan, Uden, The Netherlands), anti-phospho (Y397)-focal adhesion kinase Ab (FAK; Invitrogen), and fluorochrome-conjugated secondary Ab (Molecular Probes, Karlsruhe, Germany). Staining of actin filaments was performed using fluorescein isothiocyanate-conjugated

phalloidin (Molecular Probes). Sections were analyzed using an Olympus BX60 fluorescence microscope (Olympus GmbH, Hamburg, Germany) and AnalySIS software or a LSM 510 Meta confocal microscope (Zeiss, Jena, Germany) and Axiovision software.

LOX Expression in Mouse Skin

All animal studies were approved by the local animal ethics committee. Skh-1 hairless mice were obtained from Charles River (Wilmington) and bred in our animal facility. They had free access to acidified water and rodent chow and were kept in a 12-hour-light-dark cycle under specific pathogen-free conditions. Animals at the age of six weeks were irradiated with a UVA1 source (Sellamed Systems, Sellamed, Gevelsberg, Germany) emitting radiation between 340 and 400 nm. Mice received a dose of 10 J/cm^2 per day (=approximately five minutes exposure) and were irradiated five times per week. Sham irradiated animals were placed into the irradiation cage for identical time periods but without receiving UV irradiation. After 15 weeks, 20 hours after the last irradiation, mice were euthanized by CO_2 asphyxiation and dorsal skin biopsies were obtained for RNA isolation, and LOX mRNA expression was analyzed by real-time PCR as previously described. Five mice per group were analyzed.

LOX Expression in Human Skin

To analyze LOX mRNA expression in human skin, biopsies were used, which previously had been obtained in an independent clinical study.[27] The study was approved by the local ethics committee. The Declaration of Helsinki Principles was obeyed. Briefly, adults voluntarily planning to use sunbeds for at least 3 months had participated in this study. The participants had declared to have never used sunbeds before or had stopped using sunbeds regularly at least 18 months ago. Two 4 mm punch biopsies from buttock and neck skin (laterally) were taken 1 day after written informed consent. Then, probands began to use sunbeds according to their choice in a regular manner. Three months later another two biopsies from buttock and neck skin were collected for RNA isolation. Biopsies from four male and two female probands were used for this study. LOX mRNA expression was assessed by real-time PCR as previously described.

Statistics

For all measurements data are expressed as mean ± SEM. The statistical significance of the differences between groups was calculated with Student's *t*-test. Differences were considered significant when $P < 0.05$.

Results

Characterization of KSS Skin Fibroblasts

In initial experiments we sought to confirm that KSS fibroblasts constitutively carry increased levels of UV-inducible large scale deletions of mtDNA as compared with NHF. For this purpose, primary skin fibroblasts from two different KSS patients and two different healthy volunteers were analyzed by semiquantitative real-time PCR for the presence of the common deletion.[26] KSS patients and healthy volunteers were age-matched and NHF and KSS fibroblasts were always used at identical passage numbers in these and all subsequent experiments. As is shown in Figure 1A, KSS fibroblasts carried significantly increased levels of the common deletion as compared with NHF. In addition, increased burden of mtDNA deletions was associated with an increased production of ROS in the cytosol and the mitochondrial compartment of KSS cells as determined by DCF and MitoSOX staining, respectively (Figure 1, B and C).

Collagen Gel Contraction by KSS Fibroblasts

We next assessed whether KSS cells—similar to NHF—were capable of forming dermal equivalents if they were seeded into collagen gels. In this system, fibroblasts contract the collagen gels within several days to form a dermal equivalent, a process that is accompanied by reorganization and remodeling of the collagen matrix.[28]

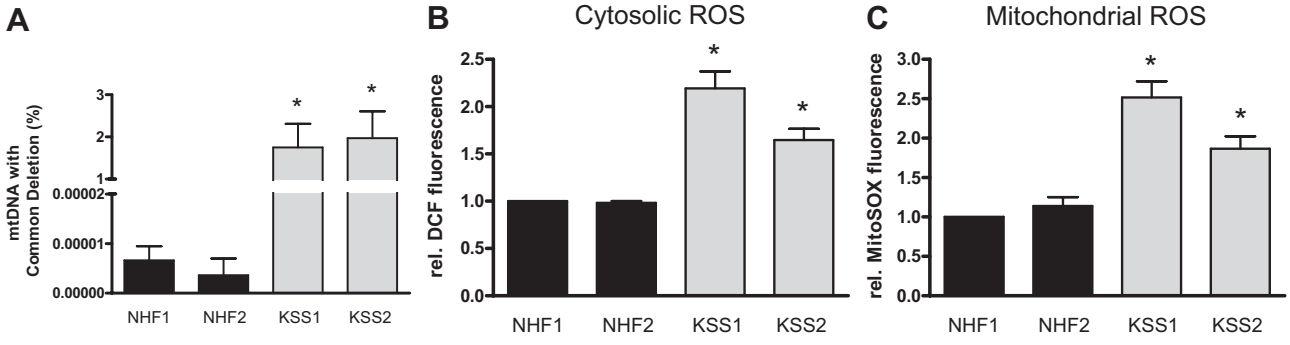

Figure 1. Increased levels of mtDNA deletions are associated with increased ROS levels in KSS fibroblasts. NHF and KSS fibroblasts of two different donors each were cultured as described in the *Materials and Methods*. **A:** Fibroblasts were harvested and DNA was isolated. Abundance of deleted mtDNA was measured on the basis of the Common Deletion, in comparison with undeleted mtDNA by real-time PCR. Data are means ± SEM of six independent experiments. DCF (**B**) and MitoSOX (**C**) fluorescence were measured in a microplate reader. Data are means ± SEM of three independent experiments. Statistically significantly different compared with both NHF, $*P < 0.05$.

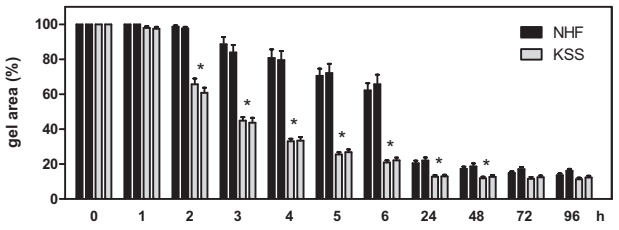

Figure 2. Increased collagen gel contraction capacity of fibroblasts with deletions of the mtDNA. NHF and KSS fibroblasts of two different donors each were seeded into collagen gels, and the gel area was determined at the various depicted time points. From the start of the experiment, the gel area was set to 100%. Data are means ± SEM of eight independent experiments. Statistically significantly different for both KSS compared with both NHF equivalents, $^{*}P < 0.05$.

Surprisingly, KSS skin fibroblasts did not only contract the collagen gels, but did so significantly faster than NHF. As is shown in Figure 2, this difference is greatest between 2 to 48 hours after the cells have been seeded into the collagen gels, whereas at later time points it becomes less and eventually the surface areas of the contracted gels are no longer different between KSS and NHF. We next asked whether the increased contraction capacity of KSS fibroblasts was related to increased ROS production by these cells. To address this question, KSS and NHF were kept under hypoxic conditions and subsequently assessed for their capacity to contract collagen gels in a hypoxic atmosphere. As is shown in Figure 3A, the previously observed contraction difference between KSS and NHF cells was clearly reduced under hypoxic conditions (Figure 3A). The inhibitory effect of oxygen depletion on contraction was more pronounced in KSS equivalents during the first 6 hours of contraction. For instance, after 6 hours, oxygen depletion led to a 100% increased gel area among KSS equivalents, while an increase of only ≈30% was noted for the oxygen-depleted NHF equivalents. Moreover, under normoxic conditions, addition of the antioxidant PBN reduced the contraction difference between NHF and KSS equivalents by inhibiting contraction of KSS fibroblasts (Figure 3B). In contrast, contraction of NHF equivalents was not affected by PBN during the first 6 hours of the contraction phase. Taken together these results indicate that the increased capacity of KSS fibroblasts to contract collagen gels is a consequence of increased ROS production by these cells and depends on the availability of oxygen.

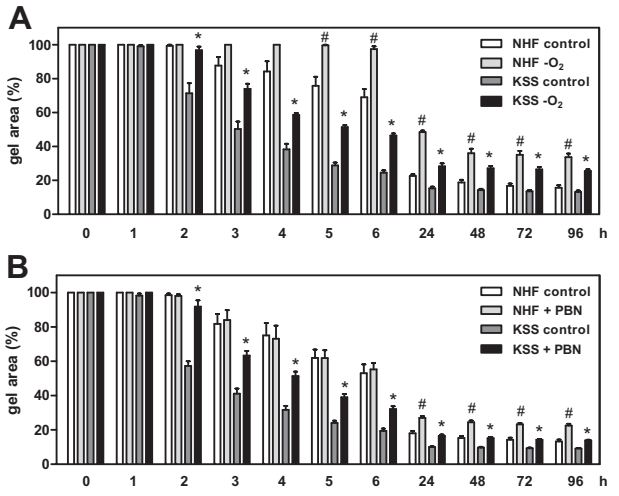

Figure 3. Increased contraction capacity of KSS fibroblasts depends on increased ROS production. **A:** NHF and KSS fibroblasts of two different donors were incubated for 48 hours in an oxygen-free environment before they were seeded into collagen gels using oxygen-deprived media. The area of the gels was determined at the various depicted time points. Shown is the relative gel area of the equivalents compared with time point 0. Data are means ± SEM of three independent experiments with pooled results for both NHF and KSS equivalents. **B:** NHF and KSS fibroblasts of two different donors each were seeded into collagen gels in the presence of 10 mmol/L PBN or control medium and the gel area was determined at various time points. Data are means ± SEM of three independent experiments with pooled results for both NHF and KSS equivalents. Statistically significantly different compared with KSS controls, $^{*}P < 0.05$. Statistically significantly different compared with NHF controls, $^{\#}P < 0.05$.

Role of LOX in Collagen Gel Contraction

We next sought to determine the cellular mechanism through which ROS-induced collagen gel contraction was mediated in KSS cells. In this regard it is of interest that the copper- and oxygen-dependent enzyme LOX has previously been implicated to play an important role in extracellular matrix stability.[29,30] Accordingly, LOX catalyzes the oxidation of peptidyl lysine side chains of certain proteins to yield α-aminoadipic-δ-semialdehyde. These aldehydes can spontaneously form condensation products with each other or a lysine residue thereby cross-linking two proteins. The condensation products undergo further non-enzymatically rearrangements resulting in the formation of stable end products like pyridinoline (Pyd) or deoxypyridinoline allowing covalent crosslinking of molecules like collagen and elastin in the extracellular matrix.[31,32] Since LOX activity is an indispensable prerequisite for collagen gel contraction,[33] we next assessed LOX expression in KSS and NHF cells. We have found that KSS fibroblasts are characterized by increased LOX mRNA (Figure 4A) and protein (Figure 4, B and C) expression. To determine whether increased LOX levels were of functional relevance for the contraction difference between KSS and NHF cells, we performed additional contraction experiments with the LOX inhibitor BAPN. In the presence of BAPN, the previously recognized enhanced collagen gel contraction capacity of KSS fibroblasts was reduced to a similar extent as previously observed under hypoxic conditions or on treatment with PBN (Figure 5). As noted before, this effect was seen best between 2 and 6 hours after beginning of contraction. Moreover, increased LOX expression appeared to be associated with increased LOX activity because compared with NHF, collagen gels containing KSS cells showed enhanced staining for Pyd crosslinks 6 hours after the beginning of the contraction process as revealed by immunofluorescence analysis (Figure 6A). Interestingly, Pyd crosslinks were mainly located in the cytoplasm of the fibroblasts. This finding supports the results of previous studies indicating additional intracellular functions of LOX apart from its well-established role in stabilizing the extracellular matrix.[34–36] As it is also well known that LOX regulates phosphorylation of FAK,[35,37,38] we analyzed the phosphorylation status of FAK at ty-

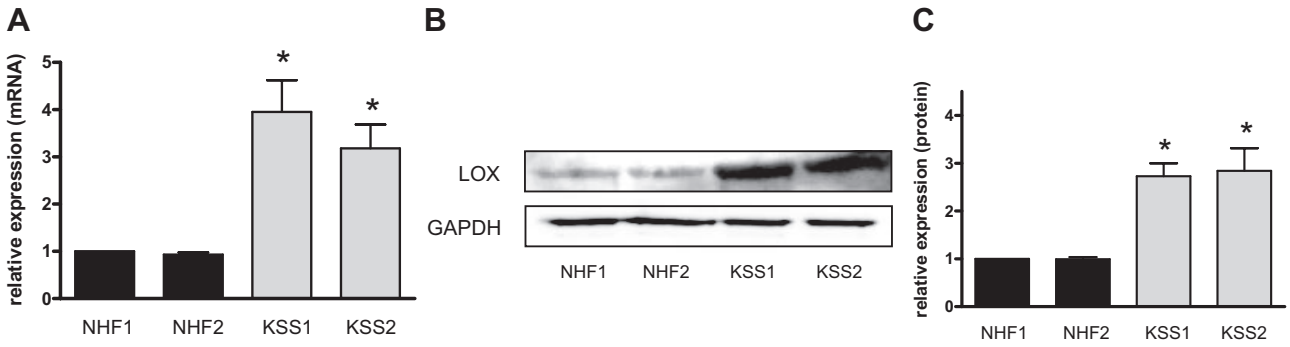

Figure 4. Increased lysyl oxidase expression in KSS fibroblasts. NHF and KSS fibroblasts of two different donors each were cultured as described in *Materials and Methods*. **A:** Cells were harvested and RNA was extracted. The LOX transcript was detected by semiquantitative real-time PCR. Expression was normalized to 18S RNA. Data are means ± SEM of five independent experiments. **B:** Western blot analysis of LOX expression in NHF and KSS fibroblasts. **C:** Densitometric analysis of LOX expression in NHF and KSS fibroblasts. Data are means ± SEM of four independent experiments. Statistically significantly different compared with both NHF, $^{*}P < 0.05$.

rosine 397. Compared with NHF KSS fibroblasts showed increased FAK phosphorylation in the equivalent (Figure 6A). Treatment with the LOX inhibitor BAPN led to a dramatic reduction of Pyd crosslink formation in the KSS equivalents while the crosslinks were only moderately reduced in NHF equivalents. In parallel, phosphorylation of FAK was reduced by BAPN and similar to the decrease of Pyd crosslinks this effect was also more pronounced in KSS fibroblasts. Finally, treatment with the antioxidant PBN reduced LOX activity in collagen gels seeded with KSS fibroblasts, as indicated by the reduced staining intensity for Pyd crosslinks and decreased phosphorylation of FAK (Figure 6A). In contrast to BAPN, PBN had no clear inhibitory effect on Pyd crosslink formation and FAK phosphorylation at tyrosine 397 in NHF equivalents reflecting our data from contraction experiments (Figure 3B and Figure 5).

A recent paper indicated a role for LOX in the regulation of actin filament polymerization. The authors demonstrated an increase in phalloidin staining in breast cancer cells on LOX inhibition.[36] To determine whether actin filament polymerization was affected in NHF and KSS equivalents, we performed phalloidin staining on cryosections of equivalents harvested 6 hours after preparation. Fluorescence microscopic analysis revealed weak phalloidin staining for control equivalents while treatment with BAPN resulted in increased signal intensity for both NHF and KSS equivalents (Figure 6B). Increased phalloidin staining was also noted in KSS equivalents treated with PBN but not in NHF paralleling the results obtained for analysis of Pyd crosslink formation, FAK phosphorylation and collagen gel contraction. In aggregate, these results indicate that increased expression and activity of LOX is critical for enhanced collagen gel contraction by KSS fibroblasts and suggest that LOX activity may be regulated by ROS. They also indicate that at least in dermal equivalents increased amounts of mtDNA deletions in human skin fibroblasts translate into structural and functional changes into the surrounding collagen tissue.

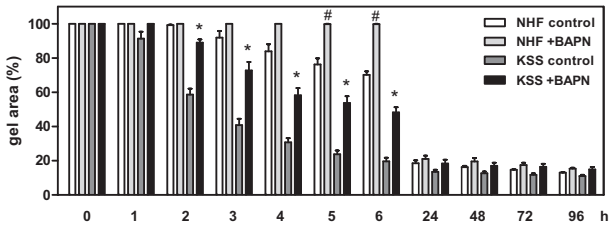

Figure 5. Enhanced collagen gel contraction of KSS fibroblasts depends on increased LOX expression. NHF and KSS fibroblasts were incubated for 24 hours in the presence of the LOX inhibitor BAPN (10 mmol/L). Then, cells were harvested and seeded into collagen gels and the area of the gels was determined at the various depicted time points. Shown is the relative gel area of the equivalents. Data are means ± SEM of three independent experiments with pooled results for both NHF and KSS equivalents. Statistically significantly different compared with KSS control, $^{*}P < 0.05$. Statistically significantly different compared with NHF control, $^{\#}P < 0.05$.

Colocalization Analysis of Pyd Crosslinks

To analyze subcellular distribution of Pyd crosslinks in more detail, we next performed colocalization experiments on cryosections of NHF and KSS equivalents harvested 6 hours after preparation. Confocal microscopy analysis confirmed increased abundance of Pyd crosslinks in KSS fibroblasts compared with NHF. Pyd crosslinks were mainly found in proximity to the plasma membrane and also in membrane protrusions, which were particularly pronounced in KSS fibroblasts (Figure 7). Additional staining for vimentin revealed a very similar distribution of this marker in NHF and KSS fibroblasts resulting in extensive colocalization with Pyd crosslinks, which was especially prominent in the membrane protrusions of the KSS fibroblasts (Figure 7A). Phalloidin staining indicated a diffuse distribution of actin filaments throughout the cells and colocalization with the Pyd crosslinks at the plasma membrane and within the membrane protrusions (Figure 7B). Finally, we analyzed colocalization of Pyd crosslinks and phospho-FAK (Y397), as LOX has been described to regulate FAK phosphorylation. Enhanced phosphorylation of FAK was observed in KSS fibroblasts confirming our results obtained by fluorescence microscopy (Figure 7C). Although phospho-FAK was distributed in a diffuse manner throughout the cells, increased abundance was found at distinct sites close to the plasma membrane. Interestingly, we also noted an accumulation of Pyd crosslinks at these sites resulting in extensive colocal-

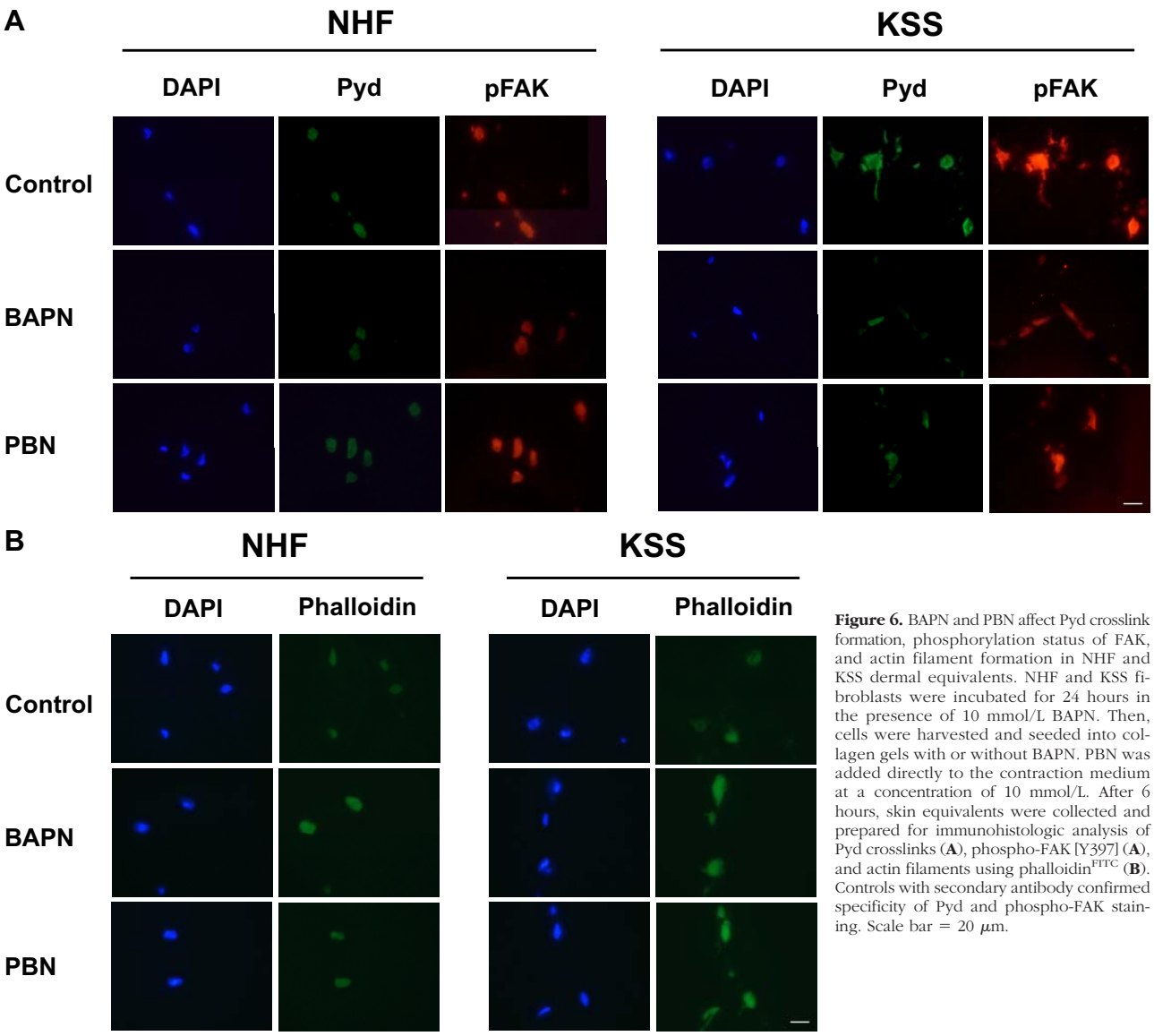

Figure 6. BAPN and PBN affect Pyd crosslink formation, phosphorylation status of FAK, and actin filament formation in NHF and KSS dermal equivalents. NHF and KSS fibroblasts were incubated for 24 hours in the presence of 10 mmol/L BAPN. Then, cells were harvested and seeded into collagen gels with or without BAPN. PBN was added directly to the contraction medium at a concentration of 10 mmol/L. After 6 hours, skin equivalents were collected and prepared for immunohistologic analysis of Pyd crosslinks (**A**), phospho-FAK [Y397] (**A**), and actin filaments using phalloidin^{FITC} (**B**). Controls with secondary antibody confirmed specificity of Pyd and phospho-FAK staining. Scale bar = 20 μm.

ization of both markers (see arrows) suggesting a link between LOX-mediated Pyd crosslink formation and FAK phosphorylation. These results indicate that intracellular structures might serve as targets for LOX-mediated Pyd crosslink formation and suggest a role for Pyd crosslinks in intracellular signaling events.

In Vivo *LOX Expression*

We therefore next wondered whether increased LOX expression can also be observed in skin *in vivo*. For this purpose, skin samples from sham-irradiated or chronically UV-exposed hairless mice, which at the time of biopsy showed significant signs of photoaging including increased wrinkle formation, reduced numbers of collagen fibers and increased expression of matrix metalloproteinase-13,[39] were analyzed for LOX mRNA expression. In all animals, LOX mRNA expression was significantly increased as compared with sham-irradiated control animals (Figure 8A). We therefore next analyzed LOX mRNA expression in skin biopsies that had been obtained in an independent study from human volunteers that were using sunbeds on a regular basis for several months. We had previously reported that in these individuals, sunbed use significantly increased the amounts of the common deletion present in their skin, as compared with the same skin site before sunbed use.[27] Here we show that an increased level of mtDNA with deletions in the skin of these individuals was associated with an increased expression of LOX mRNA (Figure 8B).

Discussion

Deletions of the mtDNA are commonly found in photoaged skin. It is however presently unclear how mtDNA deletions contribute to the premature aging process. In the present study, we assessed the capacity of skin fibroblasts derived from KSS patients harboring high levels of UV-inducible mtDNA deletions to contract a type I

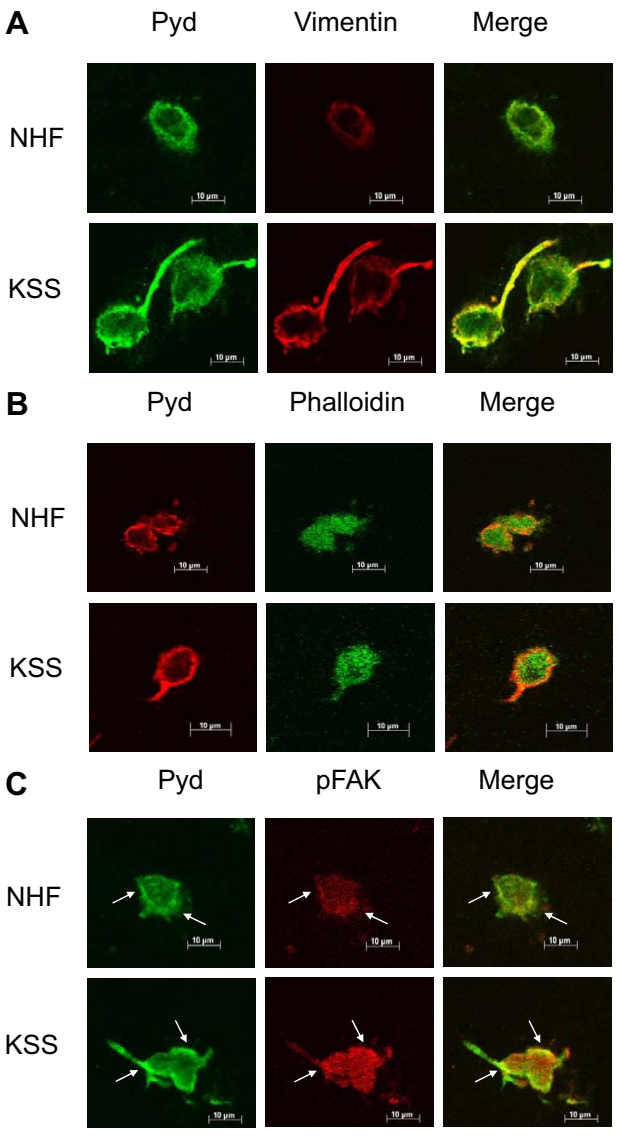

Figure 7. Colocalization analysis of Pyd crosslinks, vimentin, actin filaments, and phospho-FAK in NHF and KSS dermal equivalents. Dermal equivalents were generated as described above, harvested after 6 hours, and processed for immunohistologic analysis using antibodies specific for Pyd crosslinks in combination with an anti-vimentin antibody (**A**), phalloidin^{FITC} (**B**), or an anti-phospho-FAK [Y397] antibody (**C**). Colocalization was analyzed using confocal microscopy. Note colocalization of high intensity staining for Pyd crosslinks and phospho-FAK in NHF and KSS fibroblasts (**arrows**).

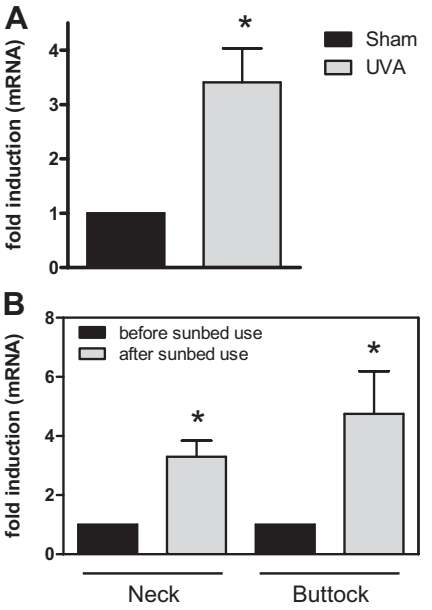

Figure 8. Increased LOX expression in the skin of UVA-irradiated hairless mice and sunbed users. **A:** Skh-1 hairless mice were chronically irradiated with an UVA1 source five consecutive days a week and received a daily dose of 10 J/cm^2. After 15 weeks, mice were euthanized and dorsal skin samples were collected for RNA isolation. LOX expression was analyzed using semiquantitative real-time PCR. Five individual mice were analyzed in both groups. Statistically significantly different compared with non-irradiated mice, $^*P < 0.05$. **B:** Biopsies from neck and buttock skin of voluntary probands intending to use sunbeds were taken before the beginning of sunbed use. During the following three months the volunteers used sunbeds according to their choice before another two biopsies of neck and buttock skin were collected. RNA was isolated from the biopsies and LOX expression was measured by semiquantitative real-time PCR. Data are means ± SEM for six probands. For each proband LOX expression in neck and buttock skin after sunbed use was normalized to the expression before sunbed use. Statistically significantly different compared with expression before sunbed use, $^*P < 0.05$.

collagen gel and form dermal skin equivalents. Fibroblasts from KSS patients were found to contract collagen gels faster and stronger than normal, healthy dermal fibroblasts. This difference, which was observed for two separate primary skin fibroblast strains from two different patients when compared with two normal fibroblast strains from two healthy donors, was not due to differences in donor age or passage number of cells. mtDNA of both KSS cell strains, however, contained significantly higher amounts of the common deletion (Figure 1). These observations indicate that the increased and accelerated collagen contraction capacity of KSS cells is due to their higher common deletion levels.

This assumption is supported by the present observation that the contraction difference between KSS and normal cells is dependent on the production of ROS. Accordingly, KSS fibroblasts showed increased ROS levels, both intramitochondrially and within the cytoplasm, and hypoxic culture conditions or treatment of cells with the antioxidant PBN abrogated the contraction difference. These results confirm and extend the findings of a previous study showing that ROS induces the reorganization and contraction of collagen gels by mesangial cells.[40] Increased intramitochondrial ROS production is thought to be a major consequence of mtDNA mutations[41–43] We therefore propose that the increased common deletion levels in KSS cells and the resulting intramitochondrial ROS production trigger a retrograde signaling cascade that affects gene expression and cellular function in KSS fibroblasts and thereby accounts for their increased capacity to contract collagen gels. In this study we have exclusively analyzed KSS cells for the presence of the common deletion, because previous studies have shown that this large scale deletion of mtDNA is UV-inducible and photoaging-associated.[10,15,17,27] We can therefore not exclude that the KSS cells used in the present study may carry additional mtDNA mutations, which may also contribute to the initiation of this signaling cascade.

At the level of gene expression, one outcome of the proposed retrograde signaling pathway is an increased

expression of LOX. Increased LOX mRNA expression in KSS cells was associated with increased protein expression and of functional relevance for the capacity of KSS cells to contract collagen gels, because KSS cells-containing dermal equivalents showed increased numbers of collagen crosslinks and chemical inhibition of LOX by the inhibitor BAPN reduced both the number of crosslinks and the collagen contraction capacity of KSS cells (Figures 5 and 6). Moreover, depletion of atmospheric oxygen, an essential substrate for LOX, also abrogated the contraction difference between KSS fibroblasts and NHF (Figure 3). Increased expression of LOX mRNA has also been observed in other cells than fibroblasts derived from patients suffering from KSS and chronic progressive external ophtalmoplegia, another disease caused by deletions of the mtDNA,[44] supporting our hypothesis that LOX expression can be induced by mtDNA deletions. Our observations are also in line with previous studies indicating a critical role of LOX in collagen gel contraction.[33,45] Crosslinking of collagen fibers also occurs during wound healing responses and increased LOX expression has been reported to occur under such conditions.[46] The present observation that human skin fibroblasts carrying large amounts of the common deletion translate into structural and functional alterations into the extracellular matrix by virtue of LOX overexpression further supports the concept that skin aging processes and wound healing responses resemble each other.[47] Interestingly, Pyd crosslinks were mainly detected in the cytoplasm of the fibroblasts suggesting that LOX is active intracellularly during collagen gel contraction. This finding is in good agreement with several other studies assessing intracellular functions for LOX.[34–37] Apparently, a major effect of intracellular LOX activity is the stimulation of migratory capacity. This process involves the indirect phosphorylation and activation of FAK[35,37,38] and is possibly also closely linked to the regulation of actin filament formation by LOX.[36] Consistent with our hypothesis that KSS fibroblasts display enhanced LOX activity, we observed increased phosphorylation of FAK at tyrosine 397 in these cells when seeded in collagen lattices. Also extensive formation of membrane protrusions was observed in KSS fibroblasts, a process that is also regulated by FAK [see ref.[48] for a review]. Either treatment with the LOX inhibitor BAPN or the antioxidant PBN reduced LOX activity in KSS fibroblasts as indicated by the decrease in Pyd crosslinks, increased actin filament formation and reduced FAK phosphorylation. This is in line with the findings of Wan et al, who showed that the treatment of fibroblasts from normal human skin or hypertrophic scars with various antioxidants could reduce the level of Pyd crosslinks[49] and Weyant et al, who demonstrated decreased FAK phosphorylation in colon cancer cells on antioxidant treatment.[50] These results suggest that enhanced LOX- and FAK-dependent migration of KSS fibroblasts might contribute at least in part to their increased capacity of contracting collagen lattices.

Confocal microscope analysis revealed high abundance of Pyd crosslinks in the membrane protrusions and in proximity to the plasma membrane of KSS fibroblasts and an extensive colocalization with phospho-FAK (Y397) at these sites. These results suggest that LOX-mediated Pyd crosslinks might play a role in FAK phosphorylation and activation. Additionally, Pyd crosslinks also largely colocalized with vimentin and partially with actin filaments. As LOX is known to be involved in the control of actin polymerization,[36] Pyd crosslinks might also be important for the regulation of this process and might additionally influence organization of the vimentin network.

In this regard it is of interest that LOX overexpression was not restricted to and thus a potential *in vitro* artifact, but instead it was observed *in vivo* in photoaged human and mouse skin as well (Figure 7). Also, increased LOX expression in human skin was associated with increased amounts of the common deletion,[27] indicating that the cause/effect relationship between mtDNA mutagenesis and LOX expression that was observed *in vitro* in dermal equivalents is of *in vivo* relevance for human skin. Our results identify LOX expression as a previously unrecognized biomarker for photoaged skin. However, they do not allow concluding whether increased LOX expression is of pathogenetic relevance for photoaging of human skin or merely an epiphenomenon. It should be noted that apart from its role in the stabilization of the extracellular matrix, additional functions of LOX have been identified. Accordingly, LOX could act as a tumor suppressor as transfection of Ha-Ras-transformed cells with LOX sense cDNA resulted in suppression of tumorigenesis when these cells were injected into athymic mice.[51] Also, LOX was shown to be essential for hypoxia-induced metastasis of breast cancer and was identified to have chemotactic properties for unstimulated human peripheral blood mononuclear cells and vascular smooth muscle cells.[37,52,53] Increased LOX expression in photoaged skin may thus additionally contribute to the development or metastasis of skin cancer, ie, a skin pathology that is known to be frequently associated with photoaging.

In conclusion, this study provides compelling evidence that human skin fibroblasts carrying large amounts of the UV-inducible common deletion in their mitochondrial genome translate functional and structural alterations into a dermal equivalent. They also suggest that this contributes to skin aging although limitations of the dermal equivalent model have to be considered when compared with the *in vivo* situation and full skin. However, under the experimental conditions of this study, ie, the use of KSS fibroblasts as a surrogate for chronically UV-irradiated cells—in dermal equivalents, these alterations appear to result from a ROS-initiated retrograde mitochondrial signaling pathway that leads to increased LOX activity. These observations further support the concept that UV-inducible large scale deletions of mtDNA are of functional relevance for photoaging of human skin.[16,54,55] Indeed, separate studies using KSS-containing dermal equivalents, which in contrast to the present study have been analyzed at later time points (>4 day-old dermal equivalents), indicate that KSS-containing dermal equivalents show several more features that are highly characteristic of photoaged human skin (Krutmann et al, manuscript in preparation).

Acknowledgments

We thank our colleague Dr. Niloofar Ale-Agha for help with the confocal microscope.

References

1. Liu Y, Fiskum G, Schubert D: Generation of reactive oxygen species by the mitochondrial electron transport chain. J Neurochem 2002, 80:780–787
2. Richter C, Park JW, Ames BN: Normal oxidative damage to mitochondrial and nuclear DNA is extensive. Proc Natl Acad Sci USA 1988, 85:6465–6467
3. Ames BN, Shigenaga MK, Hagen TM: Oxidants, antioxidants, and the degenerative diseases of aging. Proc Natl Acad Sci USA 1993, 90:7915–7922
4. Clayton DA, Doda JN, Friedberg EC: The absence of a pyrimidine dimer repair mechanism in mammalian mitochondria. Proc Natl Acad Sci USA 1974, 71:2777–2781
5. McKenzie M, Liolitsa D, Hanna MG: Mitochondrial disease: mutations and mechanisms. Neurochem Res 2004, 29:589–600
6. DiMauro S, Schon EA: Mitochondrial respiratory-chain diseases. N Engl J Med 2003, 348:2656–2668
7. Bua E, Johnson J, Herbst A, Delong B, McKenzie D, Salamat S, Aiken JM: Mitochondrial DNA-deletion mutations accumulate intracellularly to detrimental levels in aged human skeletal muscle fibers. Am J Hum Genet 2006, 79:469–480
8. Cortopassi GA, Arnheim N: Detection of a specific mitochondrial DNA deletion in tissues of older humans. Nucleic Acids Res 1990, 18:6927–6933
9. Kraytsberg Y, Kudryavtseva E, McKee AC, Geula C, Kowall NW, Khrapko K: Mitochondrial DNA deletions are abundant and cause functional impairment in aged human substantia nigra neurons. Nat Genet 2006, 38:518–520
10. Berneburg M, Grether-Beck S, Kurten V, Ruzicka T, Briviba K, Sies H, Krutmann J: Singlet oxygen mediates the UVA-induced generation of the photoaging-associated mitochondrial common deletion. J Biol Chem 1999, 274:15345–15349
11. Trifunovic A, Wredenberg A, Falkenberg M, Spelbrink JN, Rovio AT, Bruder CE, Bohlooly Y, Gidlof S, Oldfors A, Wibom R, Tornell J, Jacobs HT, Larsson NG: Premature ageing in mice expressing defective mitochondrial DNA polymerase. Nature 2004, 429:417–423
12. Kujoth GC, Hiona A, Pugh TD, Someya S, Panzer K, Wohlgemuth SE, Hofer T, Seo AY, Sullivan R, Jobling WA, Morrow JD, Van RH, Sedivy JM, Yamasoba T, Tanokura M, Weindruch R, Leeuwenburgh C, Prolla TA: Mitochondrial DNA mutations, oxidative stress, and apoptosis in mammalian aging. Science 2005, 309:481–484
13. Birch-Machin MA, Tindall M, Turner R, Haldane F, Rees JL: Mitochondrial DNA deletions in human skin reflect photo-rather than chronologic aging. J Invest Dermatol 1998, 110:149–152
14. Berneburg M, Krutmann J: Mitochondrial DNA deletions in human skin reflect photo- rather than chronologic aging. J Invest Dermatol 1998, 111:709–710
15. Berneburg M, Plettenberg H, Medve-Konig K, Pfahlberg A, Gers-Barlag H, Gefeller O, Krutmann J: Induction of the photoaging-associated mitochondrial common deletion in vivo in normal human skin. J Invest Dermatol 2004, 122:1277–1283
16. Krutmann J, Gilchrest BA: Photoaging of skin. Skin Aging. Edited by BA Gilchrest and J Krutmann. Boston, Duesseldorf, 2006, pp 33–44
17. Berneburg M, Gattermann N, Stege H, Grewe M, Vogelsang K, Ruzicka T, Krutmann J: Chronically ultraviolet-exposed human skin shows a higher mutation frequency of mitochondrial DNA as compared to unexposed skin and the hematopoietic system. Photochem Photobiol 1997, 66:271–275
18. Berneburg M, Gremmel T, Kurten V, Schroeder P, Hertel I, von Mikecz A, Wild S, Chen M, Declercq L, Matsui M, Ruzicka T, Krutmann J: Creatine supplementation normalizes mutagenesis of mitochondrial DNA as well as functional consequences. J Invest Dermatol 2005, 125:213–220
19. Bell E, Ivarsson B, Merrill C: Production of a tissue-like structure by contraction of collagen lattices by human fibroblasts of different proliferative potential in vitro. Proc Natl Acad Sci USA 1979, 76:1274–1278
20. Marionnet C, Pierrard C, Vioux-Chagnoleau C, Sok J, Asselineau D, Bernerd F: Interactions between fibroblasts and keratinocytes in morphogenesis of dermal epidermal junction in a model of reconstructed skin. J Invest Dermatol 2006, 126:971–979
21. Bernerd F, Asselineau D, Frechet M, Sarasin A, Magnaldo T: Reconstruction of DNA repair-deficient xeroderma pigmentosum skin in vitro: a model to study hypersensitivity to UV light. Photochem Photobiol 2005, 81:19–24
22. Bosca AR, Tinois E, Faure M, Kanitakis J, Roche P, Thivolet J: Epithelial differentiation of human skin equivalents after grafting onto nude mice. J Invest Dermatol 1988, 91:136–141
23. Mildner M, Ballaun C, Stichenwirth M, Bauer R, Gmeiner R, Buchberger M, Mlitz V, Tschachler E: Gene silencing in a human organotypic skin model. Biochem Biophys Res Commun 2006, 348:76–82
24. Asselineau D, Prunieras M: Reconstruction of 'simplified' skin: control of fabrication. Br J Dermatol 1984, 111 Suppl 27:219–222
25. Bernerd F, Asselineau D, Vioux C, Chevallier-Lagente O, Bouadjar B, Sarasin A, Magnaldo T: Clues to epidermal cancer proneness revealed by reconstruction of DNA repair-deficient xeroderma pigmentosum skin in vitro. Proc Natl Acad Sci USA 2001, 98:7817–7822
26. Koch H, Wittern KP, Bergemann J: In human keratinocytes the common deletion reflects donor variabilities rather than chronologic aging and can be induced by ultraviolet A irradiation. J Invest Dermatol 2001, 117:892–897
27. Reimann V, Kramer U, Sugiri D, Schroeder P, Hoffmann B, Medve-Koenigs K, Jockel KH, Ranft U, Krutmann J: Sunbed use induces the photoaging-associated mitochondrial common deletion. J Invest Dermatol 2008, 128:1294–1297
28. Genever PG, Cunliffe WJ, Wood EJ: Influence of the extracellular matrix on fibroblast responsiveness to phenytoin using in vitro wound healing models. Br J Dermatol 1995, 133:231–235
29. Kobayashi H, Ishii M, Chanoki M, Yashiro N, Fushida H, Fukai K, Kono T, Hamada T, Wakasaki H, Ooshima A: Immunohistochemical localization of lysyl oxidase in normal human skin. Br J Dermatol 1994, 131:325–330
30. Hayashi K, Fong KS, Mercier F, Boyd CD, Csiszar K, Hayashi M: Comparative immunocytochemical localization of lysyl oxidase (LOX) and the lysyl oxidase-like (LOXL) proteins: changes in the expression of LOXL during development and growth of mouse tissues. J Mol Histol 2004, 35:845–855
31. Fujimoto D: Isolation and characterization of a fluorescent material in bovine achilles tendon collagen. Biochem Biophys Res Commun 1977, 76:1124–1129
32. Ogawa T, Ono T, Tsuda M, Kawanishi Y: A novel fluor in insoluble collagen: a crosslinking moiety in collagen molecule. Biochem Biophys Res Commun 1982, 107:1252–1257
33. Woodley DT, Yamauchi M, Wynn KC, Mechanic G, Briggaman RA: Collagen telopeptides (cross-linking sites) play a role in collagen gel lattice contraction. J Invest Dermatol 1991, 97:580–585
34. Li W, Nellaiappan K, Strassmaier T, Graham L, Thomas KM, Kagan HM: Localization and activity of lysyl oxidase within nuclei of fibrogenic cells. Proc Natl Acad Sci USA 1997, 94:12817–12822
35. Payne SL, Fogelgren B, Hess AR, Seftor EA, Wiley EL, Fong SF, Csiszar K, Hendrix MJ, Kirschmann DA: Lysyl oxidase regulates breast cancer cell migration and adhesion through a hydrogen peroxide-mediated mechanism. Cancer Res 2005, 65:11429–11436
36. Payne SL, Hendrix MJ, Kirschmann DA: Lysyl oxidase regulates actin filament formation through the p130(Cas)/Crk/DOCK180 signaling complex. J Cell Biochem 2006, 98:827–837
37. Erler JT, Bennewith KL, Nicolau M, Dornhofer N, Kong C, Le QT, Chi JT, Jeffrey SS, Giaccia AJ: Lysyl oxidase is essential for hypoxia-induced metastasis. Nature 2006, 440:1222–1226
38. Laczko R, Szauter KM, Jansen MK, Hollosi P, Muranyi M, Molnar J, Fong KS, Hinek A, Csiszar K: Active lysyl oxidase (LOX) correlates with focal adhesion kinase (FAK)/paxillin activation and migration in invasive astrocytes. Neuropathol Appl Neurobiol 2007, 33:631–643
39. Cho HS, Lee MH, Lee JW, No KO, Park SK, Lee HS, Kang S, Cho WG, Park HJ, Oh KW, Hong JT: Anti-wrinkling effects of the mixture of vitamin C, vitamin E, pycnogenol, and evening primrose oil, and molecular mechanisms on hairless mouse skin caused by chronic

ultraviolet B irradiation. Photodermatol Photoimmunol Photomed 2007, 23:155–162
40. Zent R, Ailenberg M, Downey GP, Silverman M: ROS stimulate reorganization of mesangial cell-collagen gels by tyrosine kinase signaling. Am J Physiol 1999, 276:F278–F287
41. Gonzalo R, Garcia-Arumi E, Llige D, Marti R, Solano A, Montoya J, Arenas J, Andreu AL: Free radicals-mediated damage in transmitochondrial cells harboring the T14487C mutation in the ND6 gene of mtDNA. FEBS Lett 2005, 579:6909–6913
42. Jou MJ, Peng TI, Wu HY, Wei YH: Enhanced generation of mitochondrial reactive oxygen species in cybrids containing 4977-bp mitochondrial DNA deletion. Ann NY Acad Sci 2005, 1042:221–228
43. Peng TI, Yu PR, Chen JY, Wang HL, Wu HY, Wei YH, Jou MJ: Visualizing common deletion of mitochondrial DNA-augmented mitochondrial reactive oxygen species generation and apoptosis upon oxidative stress. Biochim Biophys Acta 2006, 1762:241–255
44. Alemi M, Prigione A, Wong A, Schoenfeld R, DiMauro S, Hirano M, Taroni F, Cortopassi G: Mitochondrial DNA deletions inhibit proteasomal activity and stimulate an autophagic transcript. Free Radic Biol Med 2007, 42:32–43
45. Elbjeirami WM, Yonter EO, Starcher BC, West JL: Enhancing mechanical properties of tissue-engineered constructs via lysyl oxidase crosslinking activity. J Biomed Mater Res A 2003, 66:513–521
46. Fushida-Takemura H, Fukuda M, Maekawa N, Chanoki M, Kobayashi H, Yashiro N, Ishii M, Hamada T, Otani S, Ooshima A: Detection of lysyl oxidase gene expression in rat skin during wound healing. Arch Dermatol Res 1996, 288:7–10
47. Campisi J: Senescent cells, tumor suppression, and organismal aging: good citizens, bad neighbors. Cell 2005, 120:513–522
48. Hanks SK, Ryzhova L, Shin NY, Brabek J: Focal adhesion kinase signaling activities and their implications in the control of cell survival and motility. Front Biosci 2003, 8:d982–d996
49. Wan KC, Wu HT, Chan HP, Hung LK: Effects of antioxidants on pyridinoline cross-link formation in culture supernatants of fibroblasts from normal skin and hypertrophic scars. Clin Exp Dermatol 2002, 27:507–512
50. Weyant MJ, Carothers AM, Bertagnolli ME, Bertagnolli MM: Colon cancer chemopreventive drugs modulate integrin-mediated signaling pathways. Clin Cancer Res 2000, 6:949–956
51. Contente S, Kenyon K, Rimoldi D, Friedman RM: Expression of gene rrg is associated with reversion of NIH 3T3 transformed by LTR-c-H-ras. Science 1990, 249:796–798
52. Lazarus HM, Cruikshank WW, Narasimhan N, Kagan HM, Center DM: Induction of human monocyte motility by lysyl oxidase. Matrix Biol 1995, 14:727–731
53. Li W, Liu G, Chou IN, Kagan HM: Hydrogen peroxide-mediated, lysyl oxidase-dependent chemotaxis of vascular smooth muscle cells. J Cell Biochem 2000, 78:550–557
54. Schroeder P, Gremmel T, Berneburg M, Krutmann J: Partial depletion of mitochondrial DNA from human skin fibroblasts induces a gene expression profile reminiscent of photoaged skin. J Invest Dermatol 2008, 128:2297–2303
55. Krutmann J, Schroeder P: Role of mitochondria in photoageing of human skin: the defective powerhouse model. J Invest Dermatol Symp Proc 2008, (in press)